Viscous fingering near the percolation threshold: Double-crossover phenomena

Takashi Nagatani
College of Engineering, Shizuoka University, Hamamatsu 432, Japan
and Center for Polymer Studies and Department of Physics, Boston University, Boston, Massachusetts 02215

H. Eugene Stanley
Center for Polymer Studies and Department of Physics, Boston University, Boston, Massachusetts 02215
(Received 15 June 1990)

Viscous fingering at a nonzero viscosity ratio on percolating clusters is considered to study morphological changes of patterns formed by the injected fluid in porous media. A fraction P of bonds is filled by the displaced fluid, while the others $(1-P)$ are blocked, where P is the usual percolation probability. Fluid with a low viscosity is injected into the percolating cluster filled by the displaced fluid with high viscosity. Morphological changes of patterns of the injected fluid are described in terms of crossover phenomena by making use of a four-parameter position-space renormalization-group method. It is found that when $\mu_I/\mu_D \ll (P-P_c) \ll 1$ the double crossover occurs from the diffusion-limited aggregation (DLA) on an incipient percolation cluster through the DLA on the perfect lattice to the dense structure, and when $1 \gg \mu_I/\mu_D \gg (P-P_c)$ the other double crossover appears from the DLA on an incipient percolation cluster through the invasion percolation to the dense structure, where μ_I/μ_D is the viscosity ratio and P_c the critical percolation probability.

I. INTRODUCTION

Fractal growth phenomena in pattern formation have recently attracted considerable attention.[1-11] Viscous fingering serves as one paradigm of fractal pattern formation. In its simplest form, one injects a fluid of low viscosity into a fluid of higher viscosity, using a Hele-Shaw cell.[11] In the limiting case of zero interfacial tension and zero viscosity ratio, one finds patterns that are isomorphic to the diffusion-limited aggregation (DLA). Various experiments for viscous fingering have been performed to find the fractal structure of pattern. Frequently, experiments for viscous fingering have been performed by using fluids with a nonzero viscosity ratio into porous media. In real experimental situations, various factors affect the pattern formation. Morphological changes of viscous fingers have been observed under distinct experimental conditions. For example, at a nonzero viscosity ratio the asymptotic behavior of viscous fingers must eventually cross over from the DLA fractal to the dense pattern.[12-15] Lenormand[16] found that by tuning the flow rate in porous media made of interconnected channels, the pattern of the injected fluid evolves continuously from invasion percolation to the DLA fractal. The crossover at the nonzero viscosity ratio has been recently analyzed by using the two-parameter real-space renormalization-group method.[12] To mimic the viscous fingering into porous media, the DLA model near the percolation threshold has been investigated by computational and analytical methods.[17-20] The crossover has been found from the DLA on an incipient percolation cluster (with fractal dimension 1.3) to the DLA on the perfect lattice (with fractal dimension 1.7). However, the crossover between invasion percolation and the DLA fractal has not been found.

In this paper, we consider viscous fingering at a nonzero viscosity ratio on percolating clusters to study morphological changes of patterns formed by the injected fluid in porous media. We investigate the following viscous fingering model: a fraction P of bonds is filled by the displaced fluid, while the others (1-P) are blocked, and fluid of a low viscosity is injected into the percolating cluster filled by the displaced fluid of high viscosity, where P is the usual percolation probability. We show that very interesting crossover phenomena occur by introducing a nonzero viscosity ratio into the DLA model on percolating clusters. We develop the four-parameter position-space renormalization-group method[12,21-24] to describe the morphological changes of the patterns. Above the percolation threshold, there are two characteristic lengths: the correlation length ξ_P of the percolation and the crossover length r_c from the DLA fractal to the dense cluster. They scale as follows:

$$\xi_P \approx (P-P_c)^{-\nu} , \tag{1}$$

$$r_c \approx (\mu_1/\mu_D)^{-1/\phi} , \tag{2}$$

where ν is the correlation length exponent of the percolation, P_c the percolation threshold, μ_I and μ_D the viscosities of the injected fluid and the displaced fluid, and ϕ the crossover exponent of the viscous fingering at a nonzero viscosity ratio. If $\xi_P \gg r_c \gg 1$, the double-crossover phenomena will occur from the DLA on the incipient percolation cluster through the invasion percolation to the dense structure. If $r_c \gg \xi_P \gg 1$, the other double crossover will appear from the DLA on the incipient percolation cluster through the DLA on the perfect lattice to the dense structure.

Murat and Aharony,[17] Oxaal *et al.*,[18] and Meakin *et al.*[19] proposed a model for viscous fingering in porous

media. The model was described as the DLA on the percolating clusters. By using the computer simulation, they found the fractal dimension of the DLA on an incipient percolation cluster and the crossover from the DLA on an incipient percolation cluster to the DLA on the perfect lattice. However, they did not consider the effect of the nonzero viscosity ratio on the pattern. The double-crossover phenomena were not found.

The organization of the paper is as follows. In Sec. II we apply the four-parameter position-space renormalization-group method to the pattern formation in the viscous fingering. We describe the renormalization procedure. In Sec. III we analyze the crossover phenomena between the DLA on the incipient percolation cluster, the DLA on the perfect lattice, the invasion percolation, and the dense cluster. In Sec. IV we present the summary.

II. RENORMALIZATION-GROUP APPROACH

We describe the porous medium as the percolating cluster. The viscous fingering in porous media is mimicked by that on the percolating cluster. We consider the bond percolation.[25] A bond is occupied by a fluid of high viscosity with the probability P and blocked with the probability $1-P$. The occupation of the bonds is random, independent of the occupation status. P is the usual percolation probability. One injects a fluid of low viscosity into the disordered network. If the occupation probability P is below the percolation threshold P_c, the fluid of low viscosity is not spreading into the fluid of high viscosity. On the other hand, if $P > P_c$, the fluid of low viscosity is spreading by replacing the fluid of high viscosity. In the limiting case of the infinite viscosity ratio, the viscous fingering is isomorphic to the DLA. We use an electrostatic analogy to transform the viscous fingering problem into a specific type of the resistor network. We describe the viscous fingering problem in terms of the dielectric breakdown language.[21–24] For simplicity, we consider the problem on the diamond hierarchical lattice. The position-space renormalization-group method applied to the pattern formation on the hierarchical lattice is not exact but comparatively accurate to derive the critical behavior of the system. This type of lattice is not realistic for describing a real porous medium but gives a likely morphological evolution. The crossover behavior is not affected by the lattice type qualitatively but the fractal dimension and the crossover exponent change with the use of different lattices. The diamond hierarchical lattice is constructed by an iterative generation of the base set. Each bond is occupied by the resistor of unit conductance with probability P and absent with probability $1-P$. A constant voltage is applied between the bottom and the top on the disordered diamond lattice. A growth probability proportional to the current is then assigned to the perimeter bond. The breakdown proceeds toward the top according to the growth probability. The breakdown occurs one by one. The breakdown bond has a high conductivity σ_a (>1). Without a generality, one can set the bond conductance as $\sigma_0=1$. The conductance ratio σ_0/σ_a corresponds to the viscosity ratio μ_I/μ_D.

We consider the renormalization procedure for deriving the four-parameter position-space renormalization-group equations. We derive the renormalization transformations for the occupation probability P, the percolation conductance σ_0, the surface conductance σ_s, and the conductance σ_a of the breakdown bond. Physically the surface conductance corresponds to an effective conductance of an active zone of a DLA cluster. We shall show that the four-parameter renormalization-group equations are given by

$$P' = R_P(P) , \tag{3}$$

$$\sigma_0' = R_0(P,\sigma_0) , \tag{4}$$

$$\sigma_s' = R_s(P,\sigma_0,\sigma_s,\sigma_a) , \tag{5}$$

$$\sigma_a' = R_a(P,\sigma_0,\sigma_s,\sigma_a) . \tag{6}$$

We distinguish between four types of bonds on the lattice for renormalization: (a) breakdown bonds, (b) growth bonds which are on the surface of the breakdown pattern, (c) unbroken bonds with unit conductance, and (d) empty bonds on which no current flows. The breakdown, growth, unbroken, and empty bonds are indicated by the thick, wavy, thin, and dotted lines, respectively, in the figures. See Ref. 21-24 for the details. We partition all the space into cells of size $b=2$ (b is the scale factor), each containing a single generator. After a renormalization transformation, these cells play the role of renormalized bonds. If the cell is spanned with the breakdown bonds, the cell is then renormalized to the breakdown bond. If the cell is not spanned with the breakdown bond and is nearest neighbor to the breakdown pattern, then the cell is renormalized as the growth bond. If the cell is constructed by the unbroken and the empty bonds, spanned with the unbroken bonds, and not nearest neighbor with the breakdown pattern, then the cell is renormalized as the unbroken bond. If the cell is spanned with the empty bonds, the cell is renormalized as the empty bond. The conductances of the renormalized bonds are transformed to different values after renormalization. We call the conductance of the growth bond the surface conductance. Also, we call the conductance of the unbroken bond the percolation conductance since it is consistent with the conductance of the percolating cell. We assume that the breakdown process occurs stepwise: the breakdown proceeds one by one, and more bonds than one never break down simultaneously.

We derive the renormalization transformations for the occupation probability P, the percolation conductance σ_0, the surface conductance σ_s, and the conductance σ_a of the breakdown bond. All the configurations of the cell for which it is possible to renormalize as the unbroken bond are consistent with all the spanning clusters that arise in the position-space renormalization group for bond percolation. The distinct configurations are labeled by α ($\alpha=a,b,c$) in Fig. 1. The configurational probability $C_{p,\alpha}$ with which a particular configuration α appears is given by

$$C_{p,a}=P^4, \quad C_{p,b}=4P^3(1-P), \quad C_{p,c}=2P^2(1-P)^2 . \tag{7}$$

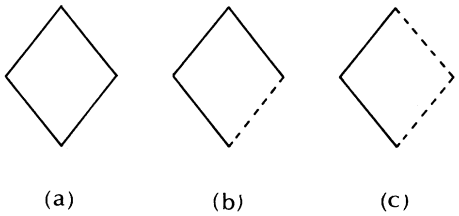

FIG. 1. All distinct configurations of the cell that it is possible to renormalize as the unbroken bond. They are consistent with all the spanning clusters arising in the bond percolation. The distinct configurations are labeled (a), (b), and (c). The unbroken and empty bonds are indicated by the thin and dotted lines, respectively.

The renormalized occupation probability P' is given by

$$P'=R_P(P)=\sum_{\alpha} C_{p,\alpha}=2P^2-P^4 , \tag{8}$$

where $R_P(P)$ is the probability that a cell of size $b=2$ is connected between the entrance and the exit.[26] This has two trivial fixed points $P=0,1$ and one nontrivial fixed point $P_c=(\sqrt{5}-1)/2$. The conductance $\sigma'_{0,\alpha}$ of the cell with the configuration α is renormalized as follows:

$$\sigma'_{0,a}=\sigma_0, \quad \sigma'_{0,b}=\sigma_0/2, \quad \sigma'_{0,c}=\sigma_0/2 . \tag{9}$$

The renormalized conductance σ'_0 of the unbroken bond will be assumed to be given by the mean value

$$\sigma'_0=R_0(P,\sigma_0)=C_{p,a}\sigma_{0,a}+C_{p,b}\sigma_{0,b}+C_{p,c}\sigma_{0,c} . \tag{10}$$

Below the percolation threshold, the conductance of the unbroken bond approaches eventually to zero. Above the percolation threshold, the conductance of the unbroken bond approaches eventually to a finite value dependent upon the occupation probability P. In previous papers,[21-24] we used the most probable value instead of the mean value. In such a case as the percolation, the most probable value does not give a likely behavior for the renormalized conductance. The most probable value does not approach eventually to zero below the percolation threshold. We here used the mean value for the renormalized conductance to approach eventually to zero below the percolation threshold.

Figure 2 shows all the configurations of the cell for which it is possible to renormalize as the growth bond. The distinct configurations are labeled by (α,β) $(\alpha,\beta=a,b,c)$. Consider the configurational probability $C_{\alpha,\beta}$ with which a particular configuration (α,β) appears. The configuration (a,b) is constructed by adding a breakdown bond to the configuration (a,a). In addition, by adding a breakdown bond to the configuration (a,b), the configuration (a,c) occurs. The configurational probabilities $C_{a,b}$ and $C_{a,c}$ are given by

$$\begin{aligned} C_{a,b}&=C_{a,a}(P_{a,a,1}+P_{a,a,2}) , \\ C_{a,c}&=C_{a,b}P_{a,b,2} . \end{aligned} \tag{11}$$

The summation of the configurational probabilities $C_{a,a}$, $C_{a,b}$, and $C_{a,c}$ equals the configurational probability $C_{p,a}$ of the spanning cluster in Fig. 1(a). The configurational probability $C_{a,a}$ is given by

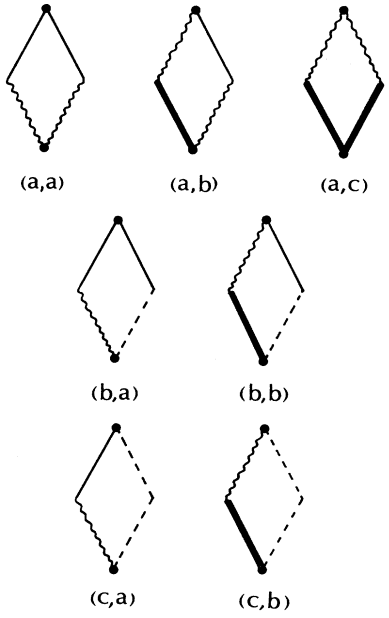

FIG. 2. All distinct configurations of the cell that it is possible to renormalize as the growth bond. The distinct configurations are labeled (a,a), (a,b), (a,c), (b,a), (b,b), (c,a), and (c,b). The breakdown, growth, unbroken, and empty bonds are indicated by the thick, wavy, thin, and dotted lines, respectively.

$$C_{a,a}+C_{a,b}+C_{a,c}=C_{p,a} . \tag{12}$$

Similarly, the configuration (b,b) is constructed by adding a breakdown bond to the configuration (b,a). The configurational probability $C_{b,b}$ is given by

$$C_{b,b}=C_{b,a} . \tag{13}$$

The sum of the configurational probabilities $C_{b,a}$ and $C_{b,b}$ equals the configurational probability $C_{p,b}$ of the spanning cluster in Fig. 1(b)

$$C_{b,a}+C_{b,b}=C_{p,b} . \tag{14}$$

Similarly, the configurational probabilities $C_{c,a}$ and $C_{c,b}$ are given by

$$C_{c,b}=C_{c,a} , \tag{15}$$

$$C_{c,a}+C_{c,b}=C_{p,c} . \tag{16}$$

Here $C_{p,a}$, $C_{p,b}$, and $C_{p,c}$ are given by (7).

The growth probability $p_{\alpha,\beta,i}$ on the growth bond i within the cell (α,β) is proportional to the current on the growth bond. Consider the resistor network problem for cells which can be renormalized as the growth bond. In the configuration labeled by (α,β) (see Fig. 2), the growth probabilities $p_{\alpha,\beta,i}$ of the growth bond i are given by

$$
\begin{aligned}
&p_{a,a,1}=p_{a,a,2}=\tfrac{1}{2}\ ,\\
&p_{a,b,1}=\sigma_a(\sigma_0+\sigma_s)/[\sigma_a(\sigma_0+\sigma_s)+\sigma_0(\sigma_a+\sigma_s)]\ ,\\
&p_{a,b,2}=1-p_{a,b,1}\ ,\\
&p_{a,c,1}=p_{a,c,2}=\tfrac{1}{2}\ ,\\
&p_{b,a}=1\ ,\\
&p_{b,b}=1\ ,\\
&p_{c,a}=1\ ,\\
&p_{c,b}=1\ .
\end{aligned}
\tag{17}
$$

The conductance $\sigma_{s,\alpha,\beta}$ of the cell with the configuration (α,β) is renormalized as follows:

$$
\begin{aligned}
&\sigma'_{s,a,a}=2\sigma_0\sigma_s/(\sigma_0+\sigma_s)\ ,\\
&\sigma'_{s,a,b}=\sigma_a\sigma_s/(\sigma_a+\sigma_s)+\sigma_0\sigma_s/(\sigma_0+\sigma_s)\ ,\\
&\sigma'_{s,a,c}=2\sigma_a\sigma_s/(\sigma_a+\sigma_s)\ ,\\
&\sigma'_{s,b,a}=\sigma'_{s,c,a}=\sigma_0\sigma_s/(\sigma_0+\sigma_s)\ ,\\
&\sigma'_{s,b,b}=\sigma'_{s,c,b}=\sigma_a\sigma_s/(\sigma_a+\sigma_s)\ .
\end{aligned}
\tag{18}
$$

The renormalized conductance σ'_s of the growth bond will be assumed to be given by the mean value

$$
\begin{aligned}
\sigma'_s=&C_{a,a}\sigma'_{s,a,a}+C_{a,b}\sigma'_{s,a,b}+C_{a,c}\sigma'_{s,a,c}\\
&+(C_{b,a}+C_{c,a})\sigma'_{s,b,a}+(C_{b,b}+C_{c,b})\sigma'_{s,b,b}\ .
\end{aligned}
\tag{19}
$$

The relationships (18) and (19) present the renormalization-group equation for the surface conductance $\sigma'_s=R_s(P,\sigma_0,\sigma_s,\sigma_a)$.

We consider the renormalization of the conductance σ_a of the breakdown bond. Figure 3 shows all the spanning clusters to be renormalized as the breakdown bond. Configurations (1)–(5) of the spanning cluster on the bottom side are constructed from the configurations of the growth cell on the top side. Configuration (1) is constructed by adding the breakdown bond onto the growth bond 1 in configuration (a,b) in Fig. 2. Configuration (2) is constructed from configurations (a,c) or (1). Configuration (3) appears from configuration (2). The configurational probabilities $C_{a,1}$, $C_{a,2}$, and $C_{a,3}$ are given by

$$
\begin{aligned}
&C_{a,1}=C_{a,0}p_{a,b,1}C_{a,b}\ ,\\
&C_{a,2}=C_{a,0}C_{a,c}+C_{a,1}\ ,\\
&C_{a,3}=C_{a,2}\ ,\\
&C_{a,1}+C_{a,2}+C_{a,3}=C_{p,a}\ .
\end{aligned}
\tag{20}
$$

Configurations (4) and (5) are constructed from configurations (b,b) and (c,b), respectively, in Fig. 2. They are given by

$$
\begin{aligned}
&C_{a,4}=C_{p,b}\ ,\\
&C_{a,5}=C_{p,c}\ .
\end{aligned}
\tag{21}
$$

The conductances $\sigma'_{a,1}-\sigma'_{a,5}$ of the cells in configurations

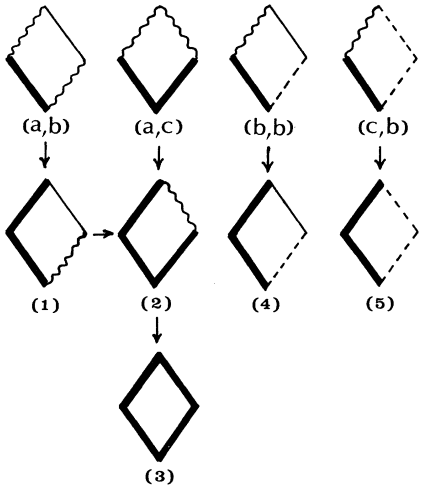

FIG. 3. All distinct configurations of the cell that it is possible to renormalize as the breakdown bond. The distinct configurations are labeled (1), (2), (3), (4), and (5). The configurations are constructed from the configurations of the growth bonds shown on the top side.

(1)–(5) are given by

$$
\begin{aligned}
&\sigma'_{a,1}=\sigma_a/2+\sigma_0\sigma_s/(\sigma_0+\sigma_s)\ ,\\
&\sigma'_{a,2}=\sigma_a/2+\sigma_a\sigma_s/(\sigma_a+\sigma_s)\ ,\\
&\sigma'_{a,3}=\sigma_a\ ,\\
&\sigma'_{a,4}=\sigma'_{a,5}=\sigma_a/2\ .
\end{aligned}
\tag{22}
$$

The renormalized conductance σ'_a of the breakdown bond will be assumed to be given by the mean value

$$
\begin{aligned}
\sigma'_a=&C_{a,1}\sigma'_{a,1}+C_{a,2}\sigma'_{a,2}+C_{a,3}\sigma'_{a,3}\\
&+(C'_{a,4}+C'_{a,5})\sigma'_{a,4}\ .
\end{aligned}
\tag{23}
$$

The relationships (22) and (23) present the renormalization-group equation for the conductance of the breakdown bond $\sigma'_a=R_a(P,\sigma_0,\sigma_s,\sigma_a)$. Equations (7)–(23) are simultaneously solved. The renormalization equations have four nontrivial fixed points $(P_c,\sigma_{0,c},\sigma_{s,c},\infty)$, $(1,1,\sigma_{\rm DLA},\infty)$, $(P_c,\sigma_{0,c},\sigma_{s,c},1)$, and $(1,1,1,1)$ in four-parameter space $(P,\sigma_0,\sigma_s,\sigma_a)$, where $\sigma_{0,c}$ is the conductance of the incipient percolation cluster, $\sigma_{s,c}$ the surface conductance at the percolation threshold when the conductance of the breakdown bond is infinite, $\sigma_{\rm DLA}$ the surface conductance on the perfect lattice. The fixed point $(P_c,\sigma_{0,c},\sigma_{s,c},\infty)$ gives the DLA fractal at the incipient percolation cluster (IPC). It is called the DLA-IPC point. The fixed point $(1,1,\sigma_{\rm DLA},\infty)$ gives the DLA fractal on the perfect lattice. It is called the DLA point. The fixed point $(P_c,\sigma_{0,c},\sigma_{s,c},1)$ gives the percolating cluster of the invasion percolation. It is called the IP point. The fixed point $(1,1,1,1)$ gives the Eden cluster on the perfect lattice. It is called the Eden point. One may expect the crossovers between the DLA fractal on incipient percolation cluster, the DLA fractal on the perfect lattice, the invasion percolation, and the Eden cluster.

III. CROSSOVER PHENOMENA

We shall find the global flow diagram in the two-parameter space $(P,\sigma_0/\sigma_a)$ in place of that in the four-parameter space for taking into account the experiment. In the experiment the physical problem could be defined by only two parameters: μ_I/μ_D and P. The conductance ratio σ_0/σ_a in the dielectric breakdown model corresponds to the viscosity ratio μ_I/μ_D in the viscous fingering. The DLA-IPC point, the DLA point, the IP point, and the Eden point in the four-parameter space are projected to $(P_c,1)$, (1,0), $(P_c,1)$, and (1,1) in the two-parameter space $(P,\sigma_0/\sigma_a)$. We set the initial values of the percolation conductance and the surface conductance as one. To find the global flow diagram in the two-parameter space, we choose a point in the parameter space, and calculate the renormalized occupation probability P', the percolation conductance σ_0', the surface conductance σ_s', and the conductance σ_a' of the breakdown bond by using Eqs. (3)–(6), to find a new point $(P',\sigma_0',\sigma_s',\sigma_a')$. We repeat this process to find the next point, and continue until we approach a stable fixed point. Figure 4 shows the renormalization flows. We can determine the stabilities of the four fixed points: the DLA-IPC point, the DLA point, the IP point, and the Eden point. The percolation transition occurs at the threshold P_c. Only above the percolation threshold does the growth process appear. The DLA-IPC point, the DLA point, and the IP point are unstable fixed points. Only the Eden point is stable in every direction. All the renormalization flows are eventually sucked into the Eden point. It is found from the flow diagram that the crossover phenomena occur from the DLA fractal on the incipient percolation cluster to the Eden cluster. The crossovers occur at two stages. If $1 \gg \sigma_0/\sigma_a \gg (P-P_c)$, the double crossover appears from the DLA fractal on the incipient percolation cluster through the invasion percolation cluster finally to the Eden cluster. The inner structure of the viscous finger shows the DLA fractal on the incipient percolation cluster on smaller length scales, the invasion percolation cluster on intermediate length scales, and the dense cluster on larger length scales. If $\sigma_0/\sigma_a \ll (P-P_c) \ll 1$, the other double crossover occurs from the DLA fractal on the incipient percolation cluster through the DLA fractal on the perfect lattice finally to the Eden cluster. The inner structure of the viscous finger shows the DLA fractal on the incipient percolation cluster on smaller length scales, the DLA fractal on intermediate length scales, and the dense cluster on larger length scales. We propose the scaling ansatz along the crossover line from the DLA-IPC point through the IP point to the Eden point,

$$M(r,P,\sigma_0/\sigma_a)=r^{d_{f,p}}F_1((\sigma_0/\sigma_a)r^{\phi_1}) \times F_2((P-P_c)r^{\phi 2}) , \tag{24}$$

with

$$F_1(x)\approx \begin{cases} 1 & \text{if } x \ll 1 \\ x^{(d_p-d_{f,p})/\phi_1} & \text{if } x \gg 1 , \end{cases} \tag{25}$$

$$F_2(x)\approx \begin{cases} 1 & \text{if } x \ll 1 \\ x^{(d-d_p)/\phi_2} & \text{if } x \gg 1 , \end{cases} \tag{26}$$

where $d_{f,p}(=1.0)$ is the fractal dimension of the DLA fractal on the incipient percolation cluster, d_p the fractal dimension of the incipient percolation cluster, d the embedding dimension, and $F_1(x)$ and $F_2(x)$ the scaling functions for the first and second crossovers. The first crossover radius, from the DLA fractal on the incipient percolation cluster to the invasion percolation cluster, scales as

$$r_{c,1}\approx(\sigma_0/\sigma_a)^{-1/\phi_1} , \tag{27}$$

where the first crossover exponent ϕ_1 is given by the value $\phi_1=1.0$ of the viscous fingering at a finite viscosity ratio on the perfect lattice.[24] The second crossover radius, from the invasion percolation cluster to the dense cluster, scales as

$$r_{c,2}\approx(P-P_c)^{-1/\phi_2} , \tag{28}$$

where the second crossover exponent ϕ_2 is given by the value $\phi_2=1/\nu$ ($\nu=1.63$) of the inverse of the correlation length exponent of percolation.[20] On the other hand, we propose the scaling ansatz along the crossover line from the DLA-IPC point through the DLA point to the Eden point,

$$M(r,P,\sigma_0/\sigma_a)=r^{d_{f,p}}F_a((P-P_c)r^{\phi_a})F_b((\sigma_0/\sigma_a)r^{\phi_b}) , \tag{29}$$

with

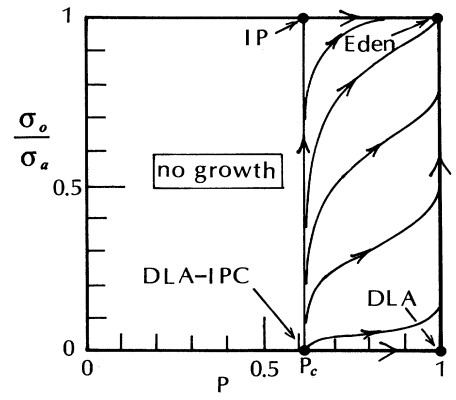

FIG. 4. Global flow diagram in the two-parameter space $(P,\sigma_0/\sigma_a)$. There are four nontrivial fixed points: the DLA-IPC point, the DLA point, the IP point, and the Eden point. All the renormalizaion flows are eventually sucked into the Eden point. The two kinds of the double-crossover phenomena appear: the first double crossover from the DLA-IPC point through the IP point to the Eden point, and the second double crossover from the DLA-IPC point through the DLA point to the Eden point.

$$F_a(x) \approx \begin{cases} 1 & \text{if } x \ll 1 \\ x^{(d_f - d_{f,p})/\phi_a} & \text{if } x \gg 1 \end{cases}, \quad (30)$$

$$F_b(x) \approx \begin{cases} 1 & \text{if } x \ll 1 \\ x^{(d - d_f)/\phi_b} & \text{if } x \gg 1 \end{cases}, \quad (31)$$

where $d_f (=1.40)$ is the fractal dimension of the DLA fractal on the perfect lattice, and $F_a(x)$ and $F_b(x)$ the scaling functions for the first and second crossovers. The value $d_f=1.40$ on the diamond hierarchical lattice is very approximate for comparing with $d_f=1.71$ of the DLA fractal on the perfect lattice. The first crossover radius, from the DLA fractal on the incipient percolation cluster to the DLA fractal on the perfect lattice, scales as

$$r_{c,a} \approx (P - P_c)^{-1/\phi_a}, \quad (32)$$

where the first crossover exponent ϕ_a is given by the value $\phi_a = 1/\nu$ ($\nu=1.63$) of the inverse of the correlation length exponent of percolation. The second crossover radius, from the DLA fractal on the perfect lattice to the dense cluster, scales as

$$r_{c,b} \approx (\sigma_0/\sigma_a)^{-1/\phi_b}, \quad (33)$$

where the second crossover exponent ϕ_b is given by the value $\phi_b = 1.0$ of the viscous fingering at a finite viscosity ratio on the perfect lattice. The above scaling relations proposed for the crossover radii remain speculative and have not been verified with the simulations.

The two kinds of double-crossover phenomena are not found in the computer simulation. In real experiments, the two-stage crossover phenomena appear frequently.[27,28] Our model shall give a prototype of the double crossover.

Here we give a comment for the result that a physical problem is defined by only two parameters: μ_I/μ_D and P. It may be difficult to relate the model parameter σ_s to the physical parameter. The parameter σ_s without a physical counterpart could be considered as a mathematical intermediate. Then the four-parameter renormalization-group equations (3)–(6) can possibly be written as the renormalization-group equations with only two parameters: σ_0/σ_a and P. The two-parameter renormalization-group equations can be obtained by dividing Eq. (6) by Eq. (4) and considering implicitly Eq. (5) as a mathematical intermediate. The result obtained from the two-parameter renormalization group is consistent with that of the global flow diagram in the two-parameter space $(P, \sigma_0/\sigma_a)$. In conclusion, the four-parameter renormalization-group method includes the two-parameter renormalization-group method.

IV. SUMMARY

We consider viscous fingering at a finite viscosity ratio on percolating clusters to study morphological changes of patterns of viscous fingers in porous media. We apply the four-parameter position-space renormalization-group method to the crossover phenomena. We find the two kinds of the double-crossover phenomena between the DLA fractal on the incipient percolation cluster, the DLA fractal on the perfect lattice, the invasion percolation cluster, and the Eden cluster. When $(P-P_c) \ll \mu_I/\mu_D \ll 1$, the double crossover occurs from the DLA fractal on the incipient percolation cluster through the invasion percolation cluster finally to the Eden cluster, where μ_I/μ_D $(=\sigma_0/\sigma_a)$ is the viscosity ratio. On the other hand, when $\mu_I/\mu_D \ll (P-P_c) \ll 1$, the other double crossover appears from the DLA fractal on the incipient percolation cluster through the DLA fractal on the perfect lattice finally to the Eden cluster. We shall give a few comments on the assumptions made in this approach and a comparison with the real experiments. The percolation probability P corresponds to the porosity in the porous media. The channels flowing fluid through porous media are not completely random but are correlated. The site-bond-correlated percolation model will be more suited to the real porous media. Also, the capillary pressure prevents the injected fluid from entering a pore. The capillary force has an important effect on the pattern formation. The capillary effect will be necessary to include in the theoretical approach. The two kinds of double-crossover phenomena have not been found in the computer simulation. The scaling Ansätze have not been verified with the simulations. The computer simulations will be necessary to include at least the two parameters: viscosity ratio and percolation probability. The large-cell renormalization-group approach will be necessary to obtain accurate fractal dimensions and accurate crossover exponents.

ACKNOWLEDGMENTS

We wish to thank Antonio Coniglio and Jysoo Lee for especially helpful conversations.

[1]T. A. Witten and L. M. Sander, Phys. Rev. Lett. **47**, 1400 (1981); Phys. Rev. B **27**, 5686 (1983).

[2]P. Meakin, Phys. Rev. A **26**, 1495 (1983); **27**, 604 (1983); **27**, 2616 (1983).

[3]*Kinetics of Aggregation and Gelation,* edited by F. Family and D. P. Landau (North-Holland, Amsterdam, 1984).

[4]*On Growth and Form,* edited by H. E. Stanley and N. Ostrowsky (Nijihoff, The Hague, 1985).

[5]*Fractals in Physics,* edited by L. Pietronero and E. Tosatti (North-Holland, Amsterdam, 1986).

[6]H. J. Herrmann, Phys. Rep. **136**, 153 (1986).

[7]P. Meakin, in *Phase Transitions and Critical Phenomena,* edited by C. Domb and J. L. Lebowitz (Academic, New York, 1988), Vol. 12, p. 336.

[8]R. Julien and R. Botet, *Aggregation and Fractal Aggregates* (World Scientific, Singapore, 1987).

[9]J. Feder, *Fractals* (Plenum, New York, 1988).

[10]*Random Fluctuations and Pattern Growth,* edited by H. E.

Stanley and N. Ostrowsky (Kluwer Academic, Dordrecht, 1988).
[11]T. Vicsek, *Fractal Growth Phenomena* (World Scientific, Singapore, 1989).
[12]J. Lee, A. Coniglio, and H. E. Stanley, Phys. Rev. A **41**, 4589 (1990).
[13]J. D. Sherwood, J. Phys. A **19**, L195 (1986).
[14]P. R. King, J. Phys. A **20**, L529 (1987).
[15]M. J. King and H. Scher, Phys. Rev. A **41**, 874 (1990).
[16]R. Lenormand, Physica (Amsterdam) **140A**, 114 (1986).
[17]M. Murat and A. Aharony, Phys. Rev. Lett. **57**, 1875 (1986).
[18]U. Oxaal, M. Murat, F. Boger, A. Aharony, and J. Feder, Nature **329**, 32 (1987).
[19]P. Meakin, M. Murat, A. Aharony, J. Feder, and T. Jossang, Physica A **155**, 1 (1989).
[20]T. Nagatani and H. E. Stanley (unpublished).
[21]T. Nagatani, Phys. Rev. A **36**, 5812 (1987); **38**, 2632 (1988).
[22]T. Nagatani, Phys. Rev. A **40**, 7286 (1989).
[23]T. Nagatani, Phys. Rev. A **41**, 994 (1990).
[24]T. Nagatani and H. E. Stanley, Phys. Rev. A **41**, 3263 (1990).
[25]D. Stauffer, *Introduction to Percolation Theory* (Taylor and Francis, London, 1985).
[26]D. C. Hong, J. Phys. A **17**, L929 (1984).
[27]V. Horvath, J. Kertesz, and T. Vicsek, Europhys. Lett. **4**, 1133 (1987).
[28]G. Daccord, O. Lietard, and R. Lenormand (unpublished).